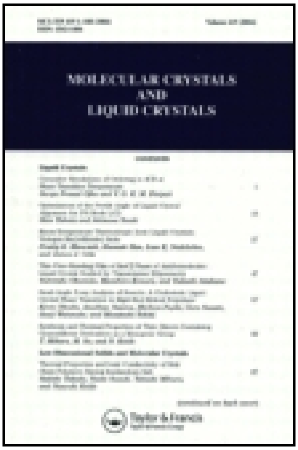

Molecular Crystals and Liquid Crystals
Publication details, including instructions for authors and subscription information:
http://www.tandfonline.com/loi/gmcl20

Thermally Stimulated Depolarization Currents and Optical Transmissionon Liquid Crystal/Cellulose Derivative Composite Devices

C. Rosu [a] , D. Manaila-Maximean [b] , M. H. Godinho [c] & P. L. Almeida [c]

[a] Department of Physics, University Politehnica Bucuresti, Splaiul Independentei 313, Bucharest, 77206, Romania

[b] LPMC, UMR 6622, Universite de Nice, Sophia Antipolis, Parc Valrose, Nice, Cedex 02, 06108, France

[c] Departamento de Ciência dos Materiais and CENIMAT, FCT/UNL, Caparica, 2829-516, Portugal

Version of record first published: 18 Oct 2010

To cite this article: C. Rosu, D. Manaila-Maximean, M. H. Godinho & P. L. Almeida (2002): Thermally Stimulated Depolarization Currents and Optical Transmissionon Liquid Crystal/Cellulose Derivative Composite Devices, Molecular Crystals and Liquid Crystals, 391:1, 1-11

To link to this article: http://dx.doi.org/10.1080/10587250216170

Mol. Cryst. Liq. Cryst., Vol. 391, pp. 1–11
Copyright © 2003 Taylor & Francis
1542-1406/03 $12.00 + .00
DOI: 10.1080/15421400390193549

THERMALLY STIMULATED DEPOLARIZATION CURRENTS AND OPTICAL TRANSMISSION ON LIQUID CRYSTAL/CELLULOSE DERIVATIVE COMPOSITE DEVICES

---

*C. Rosu**
Department of Physics—University Politehnica Bucuresti,
Splaiul Independentei 313, 77206 Bucharest, Romania

D. Manaila-Maximean
LPMC, UMR 6622, Universite de Nice—Sophia Antipolis,
Parc Valrose, 06108 Nice, Cedex 02, France

M. H. Godinho and P. L. Almeida
Departamento de Ciência dos Materiais and CENIMAT,
FCT/UNL, 2829–516 Caparica, Portugal

In this paper we examined the electrical and optical properties of a new composite device containing layers of a nematic liquid crystal and cellulose derivative. Using the thermally stimulated depolarization current (TSDC) method we obtained information regarding the conduction mechanism, the activation energy, and the pre-exponential frequency factor in the Arrhenius diagrams. The optical transmission is slightly dependent on the polarization field, and the thermal switch behavior was obtained at the nematic–isotrop transition. When a.c. voltage is applied to the sample, the optical transmission depends strongly on the field amplitude, and a very good contrast is obtained.

Keywords: nematic liquid crystals; cellulose; thermally stimulated depolarization currents; activation energy; optical transmission

Received 19 March 2002; accepted 10 September 2002.

This work was partially supported by PRAXIS XXI—FCT/MCT Portugal, under research contract POCTI/CTM/2620/95 and FEDER. P. L. Almeida wishes to thank partial support from the PRAXIS program grant no. PRAXIS XXI BD 17071/98.

*Corresponding author. E-mail: rosudanut@yahoo.com

INTRODUCTION

Field-induced thermally stimulated currents (FITSC) method [1] consists of measuring the currents generated by the build-up and/or release of a polarized state in a dielectric sandwiched between two electrodes when the sample is heated or cooled with a constant rate. The general experimental procedure usually involves four steps (Fig. 1):

1. Application of a polarizing d.c. bias voltage V_p at a temperature T_p.
2. Cooling under this bias down to a lower temperature T_0.
3. Change of the bias voltage at T_0 to another value, depolarization voltage, V_d.
4. Heating at a constant rate while maintaining the new bias and recording the current as a function of temperature.

If the depolarization voltage V_d is zero, the current peaks are observed during the thermally activated transition from the polarized state to the equilibrium one, and the method is called thermally stimulated depolarization currents (TSDC). If $V_p = 0$, the current peaks are superimposed to the normal d.c. conduction, as the result of the opposite process, i.e., thermally activated transition from the equilibrium state to the polarized state, thermally stimulated polarization currents (TSPC). The currents are due to the combined effects of polarization and depolarization mechanisms when both $V_d \neq 0$ and $V_p \neq 0$. The FITSC method is used for investigating

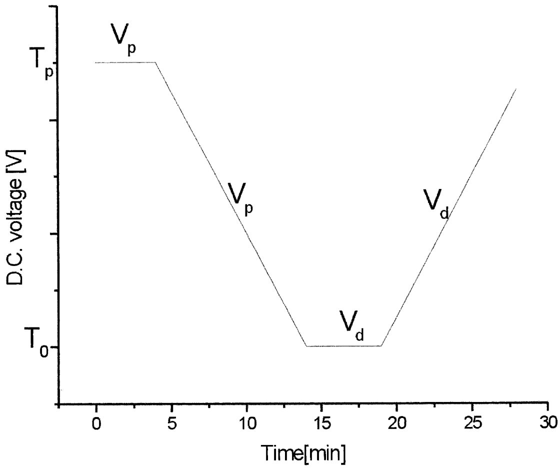

FIGURE 1 General experimental procedure for FITSC, with depolarization voltage $V_d \neq 0$ and polarization voltage $V_p \neq 0$.

the electrical properties of dielectrics via study of thermal relaxation effects and offers an attractive alternative to the conventional bridge methods, current-voltage-temperature measurements, or differential scanning calorimetry when used to study phase transitions [1–4].

In this paper we study a composite system obtained by sandwiching a layer of cellulose-based polymeric matrix in between two layers of a nematic liquid crystal [5,6]; the electro-optical properties of the resulting device are similar to those of standard PDLC systems [7–12]. They can be switched from an "OFF" state to an "ON" state. For a LC with positive dielectric anisotropy, $\Delta\varepsilon > 0$, in the field "OFF" state, surface anchoring of the LC to the polymer causes a director distortion near the rough polymeric surface [7]. Thus the film scatters light due to the mismatch between the effective refractive index n_{eff} of the LC and the refractive index of the polymer n_p. When applying an a.c. voltage, in the field ON state, the director is aligned along the field direction, $n_{eff} = n_{o(LC)}$, and for normal incidence light, the film becomes transparent if the ordinary refractive index of the LC $n_{o(LC)}$ is equal to n_p.

Using the TSDC method we obtained information regarding the conduction mechanism. Optical transmission was simultaneously measured.

EXPERIMENTAL

Sample Preparation

The cellulose derivative [13] HPC (Aldrich, $M_w = 100{,}000\,\mathrm{g\,mol^{-1}}$) was dried in vacuum at 50°C for about 48 h before use. Solid films of HPC cross-linked with 1,4-diisocyanatobutane (BDI) (7% w/w) were prepared from solutions of HPC in acetone according to the procedure described previously [5]. The refractive index of the HPC film is $n_p = 1.5$. The composite material was obtained by covering both surfaces of the solid film (20 μm thick) with 10 μm thick layers of the nematic liquid crystal E7 (commercially available from Merck, UK), with $n_{o(LC)} = 1.5121$ and $n_{e(LC)} = 1.7367$. The thickness of the liquid crystal layers was maintained using 40 μm spacers. This layered structure of the sample is different from the one in which the cellulose derivatives (cellulose acetate membranes) are impregnated with liquid crystals. The devices studied and prepared by Craighead *et al.* [15] have a lower contrast ratio than our samples [5].

Experimental Setup

Figure 2 presents the schematic experimental setup for the TSDC measurements. Using this setup the optical transmission was simultaneously measured. The analyzed sample (CL) was introduced in an oven (F).

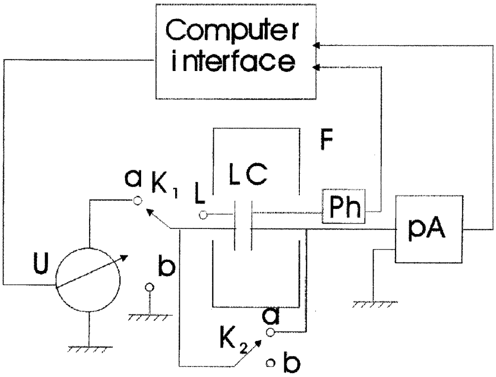

FIGURE 2 Schematic setup for FITSC and the simultaneous optical measurements.

The computer controls the heating-cooling rate and the value of the voltage (U) applied on the sample. The switches K_1 and K_2, also computer controlled, perform the different steps of the experiment in succession. When K_1 is switched on to position a (i.e. $K_1 = a$) and $K_2 = b$, the d.c. voltage U is applied on the sample; when $K_1 = b$ and $K_2 = b$, the sample is short-circuited and the picoammeter (pA), measures the current through the sample. Finally, if $K_1 = b$ and $K_2 = a$, the sample is short-circuited and the stored charges will be eliminated. Figure 3 illustrates the heating-cooling steps of the experiment. In the first heating step (0), from room temperature to a pre-established temperature (T_p) lower than the glass transition of the polymer matrix, initial depolarization of the sample takes place. During the steps 1, 2, and 3 the polarizing field $E_p = 0$; these steps are performed to eliminate the eventually existing charges, due to previous treatments applied on the sample. During step 4, at T_p, the polarizing field $E_p = V_p/g$ is applied, (where g is the thickness of the sample) and it is

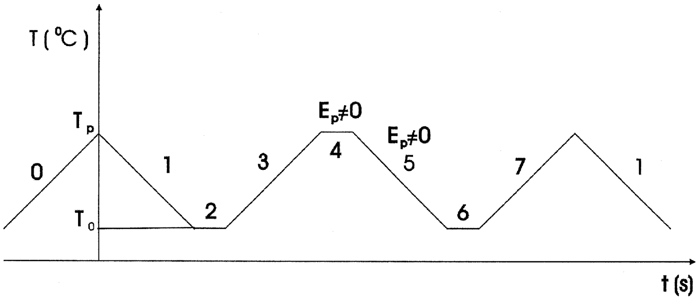

FIGURE 3 Heating-cooling cycles applied to the samples.

maintained during the cooling down to T_0 (step 5). During the phase 6, the field E_p is cut off, and the sample is short-circuited to eliminate capacitive discharge. The depolarizing currents are registered during step 7. The heating-cooling rates were of 1 K/min, and steps 2, 4, and 6 were of 15 min. In this experiment, the polarization temperature is $T_p = 95°\mathrm{C}$ and $T_0 = 25°\mathrm{C}$. The optical beam from the light source (L) is transmitted through the sample and measured by the photomultiplier (Ph); no polarizers have been used.

Independently of the above described experiment, we measured the dependence of the optical transmission coefficient on the a.c. voltage applied on the cells from a generator operating at the frequency of 1 kHz. All the electro-optical results were obtained for normal sample incidence at room temperature (23°C).

RESULTS AND DISCUSSION

According to the heating–cooling cycles presented in Figure 3, the electrical field E_p is applied to the sample at the higher temperature T_p and it is maintained constant during cooling. The polarization of the dielectrics submitted to an external electric field is due to the mechanisms involving microscopic or macroscopic charge displacement. Since the internal friction and ionic mobility depend exponentially on temperature, heating a dielectric to a high temperature T_p enhances the response time of permanent dipoles and internal free charges to the applied electric field and allows the equilibrium polarization to be reached in short time. When the polarization field is maintained while cooling the sample to a temperature T_o sufficiently low to increase the relaxation times of the dipoles and ions to values of hours or more, these are practically “frozen” in the electrical configuration reached at T_p and consequently do not respond when the field is switched off. The equilibrium polarization $P_e(T_p)$ reached during the polarization phase 5 is consequently considered constant at the end of the cooling, when the heating step begins (step 7). In step 7 the thermally induced depolarization currents are measured. In Figures 4 and 5 the thermally stimulated depolarization currents versus temperature are presented.

Considering the charge given by the Eq. (1):

$$Q = -\int_{t_1}^{t_2} i(t) \cdot dt = -\frac{dt}{dT} \cdot \int_{T_1}^{T_2} i(T) \cdot dT \qquad (1)$$

where t denotes the time and T is the temperature. We notice that the sign of the charge depends on the sign of the current, respectively on the sign of

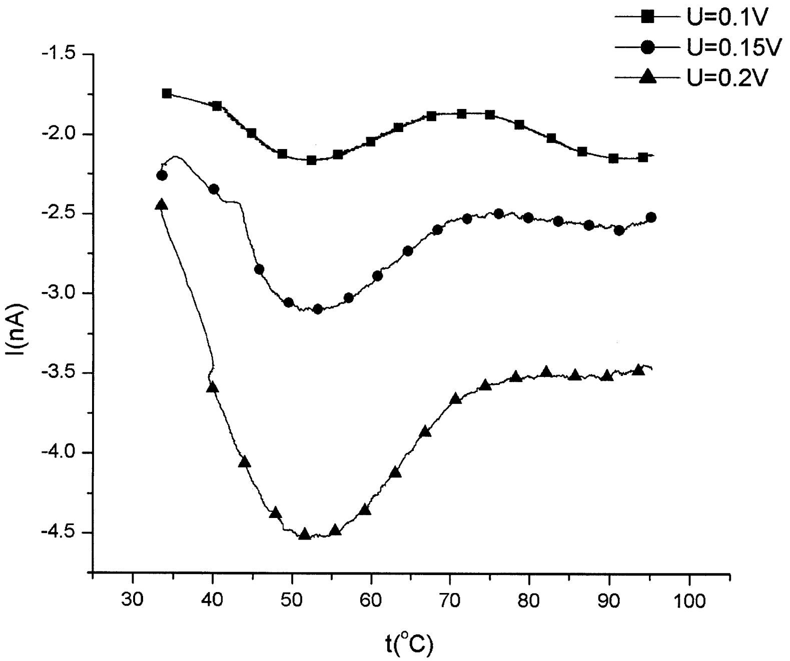

FIGURE 4 TSDC spectra for lower polarization voltages.

variation of temperature $\frac{dt}{dT}$; for step 7, the last term is positive, because the temperature is increasing.

Considering the polarity of the voltage applied on the sample positive compared to the ground, it follows that if the current is positive, it is produced by a heterocharge (with a polarity opposing that of the electrode), and if the current is negative, it is due to a homocharge.

From Figure 4 we notice that at the increase of the temperature the absolute value of the registered current increases until it reaches a maximum at $T_1 = 52°C$, at the phase transition nematic-isotropic of the liquid crystal. As expected, this value is lower than the one measured for the pure LC by the DSC or by TSDC [14], ($T_{N\text{-}I} = 60°C$), because the dipolar structure will be oriented differently by the conjugated action of the polarizing field and the LC-cellulose interactions.

The negative sign of the registered currents in step 7 is specific to homocharges. To study the conduction mechanism specific for the current, we represented in Figure 6 the peak value of this current versus the polarizing voltage. We notice a linear dependence of the peak current on the polarization voltage. As it is known (See Eq. (1)), this is characteristic for the dipolar currents (for the currents limited by the spatial charge, this

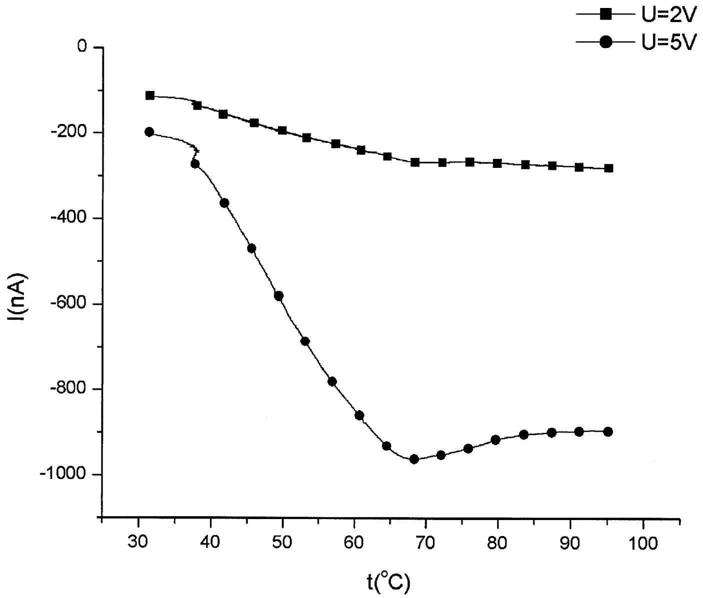

FIGURE 5 TSDC spectra for polarization voltages U = 2V and U = 5V.

dependence is nonlinear). The existence of a single peak suggests one relaxation time. The polarization of a material charged initially with the polarization $P_e(T_p)$, for which the applied field is interrupted (step 7), is given by Eq. (2):

$$\frac{dP}{dt} = -\frac{(P - P_\infty)}{\tau} \tag{2}$$

This equation supposes a relaxation proportional with the difference between the instant polarization and the polarization P_∞ reached by the sample after a sufficiently long time. Suppose that step 7 is long enough so that at its end the polarization becomes zero ($P_\infty = 0$). The proportionality factor τ from Eq. (2) is the relaxation time, supposed constant at constant temperature. The temperature dependence of the relaxation time is given by an Arrhenius equation:

$$\tau = \tau_0 \cdot exp\left(\frac{E}{k \cdot T}\right) = \frac{1}{s_0} \cdot exp\left(\frac{E}{k \cdot T}\right) \tag{3}$$

where s_0 is the frequency pre-exponential factor and E is the activation energy.

Considering that the temperature T changes according to the law:

$$T = T_0 + q \cdot t \tag{4}$$

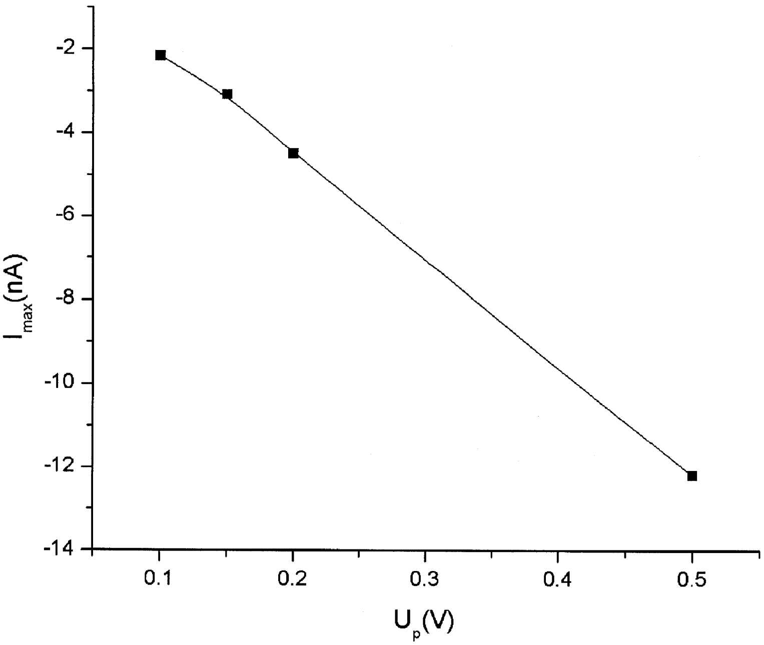

FIGURE 6 The peak value of depolarization currents obtained in step 7 versus the polarizing voltages.

where T_0 is the temperature at the beginning step 7 and $q = \frac{dT}{dt}$ is the heating rate, the relaxation time will vary: $\tau = \tau(T(t)) = \tau(t)$.

Introducing Eq. (3) into Eq. (2) and integrating we obtain:

$$\begin{aligned} P(t) &= P_e(T_p) \cdot exp\left(-\int_0^t \frac{d\theta}{\tau(\theta)} \cdot d\theta \right) \\ &= P_e(T_p) \cdot exp\left(-\int_0^t s_0 \cdot exp\left(-\frac{E}{k \cdot T(\theta)} \right) \cdot d\theta \right) \end{aligned} \tag{5}$$

Changing the variable $T = T_0 + q \cdot t$, we obtain:

$$P(t) = P_e(T_p) \cdot exp\left(-\frac{s_0}{q} \cdot \int_{T_0}^{T} exp\left(-\frac{E}{k \cdot \theta} \right) \cdot d\theta \right) \tag{6}$$

The dipolar depolarization current will be

$$J = -\frac{\partial P}{\partial t} = P_e(T_p) \cdot s_0 \cdot exp\left(-\frac{E}{k \cdot T} - \frac{s_0}{q} \cdot \int_{T_0}^{T} exp\left(-\frac{E}{k \cdot \theta} \right) \cdot d\theta \right) \tag{7}$$

In order to calculate the coefficients E and s_0, we should estimate the integral in Eq. (7); to avoid calculus difficulties, we have analyzed the dependence $f(T) = J'(T)/J(T)$, where $J'(T) = dJ(T)/dT$. This follows from

$$J'(T) = P_e(T_p) \cdot s_0 \cdot \left(\frac{E}{k \cdot T^2} - \frac{s_0}{q} \cdot exp\left(-\frac{E}{k \cdot T} \right) \right) \cdot exp\left(-\frac{E}{k \cdot T} - \frac{s_0}{q} \cdot \int_{T_0}^{T} exp\left(-\frac{E}{k \cdot \theta} \right) \cdot d\theta \right)$$

It results in

$$f = \frac{J'(T)}{J(T)} = \frac{E}{k \cdot T^2} - \frac{s_0}{q} \cdot exp\left(-\frac{E}{k \cdot T} \right) \tag{8}$$

The numerical analysis of the experimental data obtained in step 7 allows the calculus of the activation energy and the frequency pre-exponential factor. We obtained the values $E = 0.91$ eV; $s_0 = 2.1 \cdot 10^{11}\ \mathrm{s}^{-1}$. We have also calculated the value of the energy activation by the Arrhenius curve method. Representing the dependence $1\mathrm{n}(I) = f\left(\frac{1}{T}\right)$, where I is the current intensity in step 5 and T is the absolute temperature, and calculating the slope of the curve we obtained from this graphic method the value of the activation energy $E = 0.95$ eV, which is very close to the one obtained before.

The optical transmission of the sample, measured in step 7 simultaneously with the depolarization currents is presented in Figure 7. We notice that it increases with the temperature, and it has a significant increase near the nematic-isotropic phase transition. The transmission increase at the N-I phase transition because the refractive index of the LC in the isotropic phase $n_{(LC)iso}$ matches the refractive index of the polymer $n_{(LC)iso} = n_p$. This process takes place at a slightly higher temperature than the N-I phase transition temperature of the pure LC, due to the LC-cellulose interactions.

The optical transmission is slightly dependent on the polarizing fields. When a.c. voltage is applied to the sample, at constant room temperature, the optical transmission depends strongly on the field amplitude, and a very good switching ON-OFF ratio is obtained. The variation of the transmission coefficient with the applied a.c. field is shown in Figure 8. When the a.c. voltage is applied, the molecules align themselves with the electric field and the ON state is achieved [7].

We can see from the curve that the sample has a maximum transmission of 0.800, a minimum transmission of 0.009, and a contrast ratio (defined as the ratio between the maximum transmission in the transparent state and the lowest transmission in the opaque state) of 88.8. The V_{on} voltage (calculated from the voltage dependence of the transmission coefficient

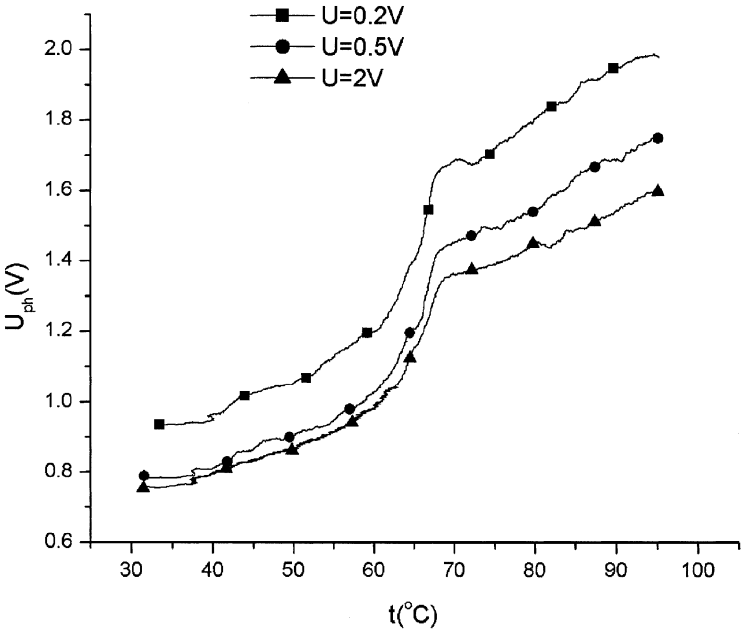

FIGURE 7 The optical signal measured by the photomultiplier in step 7.

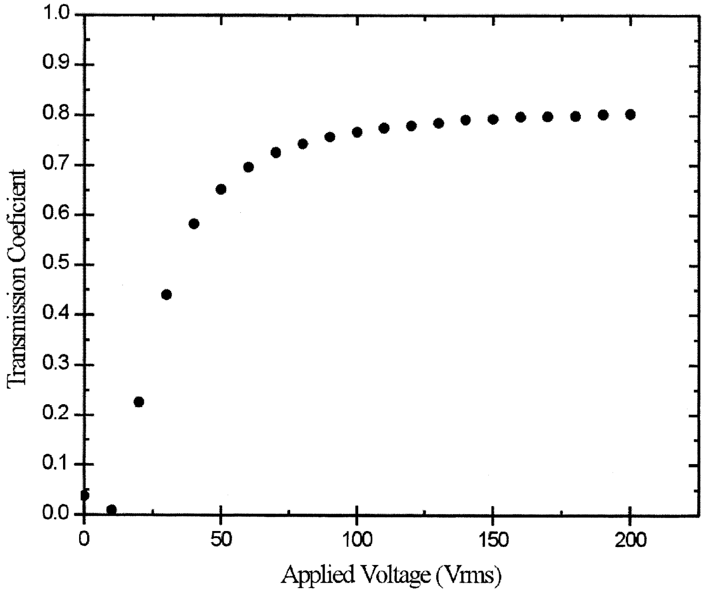

FIGURE 8 Optical transmission coefficient versus a.c. applied voltage at constant room temperature.

and representing the applied a.c. voltage necessary to reach 90% of the maximum transmission of the sample) for this sample is 69.9 V_{rms}.

CONCLUSIONS

The results of the field-induced depolarization currents measurements on this layered LC-cellulose derivative composite device show a dipolar conduction mechanism with one relaxation time. The values of the activation energy and the frequency pre-exponential factor are typical for the nematic LC, indicating that it has a major part in the conduction of the device as compared to the conduction processes in cellulose. The optical transmission measured simultaneously with the depolarization currents has a small dependence on the polarization field. The dependence of the optical transmission on the temperature has a discontinuity at the nematic-isotrop phase transition.

At constant room temperature and a.c. applied voltage, the optical transmission strongly depends on the field amplitude, with an excellent ON-OFF ratio. Thus these devices can be used in electro-optical application, where the noise immunity is essential.

REFERENCES

[1] van Turnhout, J. (1975). *Thermally Stimulated Discharge of Polymer Electrets.* Amsterdam: Elsevier.
[2] Sharma, R. & Sud, L. V. (1981). *J. Phys. D: Appl. Phys.*, *14*, 1671–1676.
[3] Costa Ribeiro, J. (1950). *An. Acad. Brasil. Cienc.*, *22*, 325.
[4] Manaila-Maximean, D., Furlani, M., Bena, R., Mellander, B. E., Rosu, C., Pop, T., & Motoc, C. (1999). *Mod. Phys. Lett. B.*, *13*(21), 759–767.
[5] Godinho, M. H., Martins, A. F., & Figueirinhas, J. L. (1996). *Liq. Cryst.*, *20*(3), 373.
[6] Almeida, P. L., Cidade, M. T., Godinho, M. H., Ribeiro, A. C., & Figueirinhas, J. L. (2001). *Mol. Cryst. Liq. Cryst.*, *359*, 79–88.
[7] Almeida, P. L., Godinho, M. H., Cidade, M. T., & Figueirinhas, J. L. (2001). *Mol. Cryst. Liq. Cryst., 368*, 121.
[8] Fergason, J. L. (1985). *SID Int. Symp. Digest Tech. Papers, 16*, 68.
[9] Doane, J. W., Vaz, N. P., Wu, B.-G., & Zumer, S. (1986). *Appl. Phys. Lett.*, *48*, 269.
[10] Doane, J. W. (1990). In: *Liquid Crystals—Applications and Uses*, Bahadur, B. (ed.). Singapore: World Scientific Publishing, Vol. 1, 361.
[11] Kitzerow, H. S. (1994). *Liquid Crystals, 16*(1), 1.
[12] Klosowicz, S. & Zmija, J. (1995). *Optical Engineering*, *34*(12), 3440–3450.
[13] Werbowyj, R. S. & Gray, D. G. (1980). *Macromolecules, 13*, 69.
[14] Manaila-Maximean, D., Bena R., Furlani, M., & Rosu, C. (2001). *Mol. Cryst. Liq. Cryst.*, *365*, 645–653.
[15] Craighead, H. V., Cheng, J., & Hackhood, S. (1982). *Appl. Phys. Lett.*, *40*, 22.